Effect of Reinforcement Type on the Tension Stiffening Model of Ultra-High Performance Concrete (UHPC)

S. Khaksefidi[1] and M. Ghalehnovi[2*]

1. Ph.D. Candidate, Department of Civil Engineering, Ferdowsi University of Mashhad, Mashhad, Iran
2. Associate Professor, Department of Civil Engineering, Ferdowsi University of Mashhad, Mashhad, Iran

Corresponding author: Ghalehnovi@um.ac.ir

ABSTRACT

Ultra-high performance concrete (UHPC) is a developing concrete and today is increasing to interest using it in structures due to its advantages such as high-compressive strength, modulus of elasticity, high durability and low-permeability. Therefore, it is necessary to provide models for the prediction of nonlinear behaviour of this material. This study is aimed to investigate the tension-stiffening phenomenon for UHPC and to propose a model for the post-cracking behaviour of the reinforced concrete members under tension. For this purpose, in this study, 24 cylindrical concrete specimens reinforced with a rebar in its center were prepared using UHPC and Two rebar types, including steel and GFRP (Glass Fiber Reinforced Polymer). Three specimen diameters (65 mm, 100 mm, and 125 mm), and two rebar diameters (12 mm and 16 mm) were considered. All specimens were tested under direct tension. According to the experimental data, a tension-stiffening model was proposed for UHPC. The proposed model has a suitable correlation with experimental results.

1. Introduction

The concrete industry is producing materials with high performance. In this context, most attempts are focused on increasing the ultimate strength of the cement-based materials and their perdurability. The result of the attempts is the production of a class of Portland cement-based materials known as ultra-high performance concrete (UHPC). UHPC is a new class of concretes, which is developed recently; that it has unique features including very high compressive strength and long-term durability compared

to ordinary concretes. UHPC is a very suitable material to produce thin structures such as narrow supports, delicate and specific structures. Using UHPC, it provides new facilities to construct tall buildings and bridges. The use of this kind of concrete has economic advantages, such as protection of reinforcement, decreasing in section's dimensions and reduction of shipment costs. Besides, the high-strength and considerable capacity of force resistance of UHPCs are provided with the novel applications for prefabricated segments [5-7].

On the other hand, FRPs due to high ratios of strength to weight and stiffness to weight are a suitable material for structural construction [2]. Difference between the mechanical properties of the FRP and steel reinforcement is a linear elastic behaviour up to failure and lower modulus of elasticity that presents the lack of plasticity in the behaviour of FRP [20]. Therefore, it is necessary to identify the nonlinear behaviour of UHPCs in combination with various types of rebars and propose a suitable model for tension stiffening behaviour in the tension areas of UHPC members for nonlinear analysis of complicated structures using the finite element analysis. There are many research reports that have been published in the past years about the tension stiffening effect of ordinary concrete members reinforced by steel. The results showed that the members have considerable tension stiffening capacity [9,21]. With the investigation of the post-cracking behaviour of the reinforced concrete specimens, researchers proposed a curve with an exponential decline branch in this region in which the exponential reduction parameter is a function for the reinforcing steel to the concrete modulus of elasticity ratio (n) and reinforcement ratio (ρ). The studies by Ebead and Marzouk [12] also led to a tension

stiffening model for concrete reinforced with FRP (Fiber Reinforced Polymer) plates that can be used in the analysis of two-way slabs reinforced with FRP plates. Ghalehnovi [14] studied the effect of steel rebar corrosion on tension stiffening behaviour. A Tension test performed on the cylindrical specimens with the length 1000 mm, made of concrete with the strength 26 MPa and with a center rebar. Studying the tension stiffening and bond-slip behaviour of normal concretes reinforced with FRP, Bana et al. [8] offered a numerical model. In a report by Elfgren and Noghabai [9], the results of the studies of seven groups of researchers on tension stiffening of reinforced concrete examined and cover thickness, the distance of cracks, the grade of rebars, tension stiffening of the rebars with no cover and the concrete softening effect on 50 tests considered as studied parameters. Eligehausen et al. [13] examined the cracking mechanism, effect of cover thickness size and diameter of rebar on cracking. Stramandinoli and Rovere [21] proposed a tension stiffening model with an exponential decline branch to be used in a computational program to analyze reinforced concrete beams. Lee and Kim [15] performed a direct tensile test on 35 specimens and examined the effect of the compressive strengths on tension stiffening and cracking behaviour of specimens. Marzouk and Chen [16] proposed an equation for the post-cracking region of ordinary and high performance concretes. Rahdar and Ghalehnovi [18] proposed a suitable model for tension stiffening of UHPC specimens reinforced with steel rebars based on the test results in the post-cracking region. Tang [22] studied the local bond behaviour of reinforcing bars in lightweight aggregate concrete (LWAC). Increasing the compressive strength, the ultimate bond strength increases. Yoo et al. [23] simulated

the flexural behaviour of beams, made of ultra-high performance fiber reinforced concrete (UHPFRC) and steel and glass fiber-reinforced polymer (GFRP) rebars. Deng et al. [10] conducted the pull-out test to investigate the bond behaviour of high strength rebar in reactive powder concrete (RPC). Saleem et al. [19] conducted pull-out and flexure tests with HSS rebar in UHPC. Nematzadeh and Poorhossein [17] studied the estimating properties of reactive powder concrete containing hybrid fibers using UPV.

2. Introduction of Tension Stiffening

In 1909, Morsh showed that, in the location of the crack, rebars bear all applied tensile force, but in the distance between neighbouring cracks, concrete can resist a part of tensile stresses through the stresses transferred from the rebars, and contribute to the tensile capacity of the member [1]. In this case, the stiffness of the reinforced concrete member after the crack is larger than rebars with no concrete cover in a certain mean strain. The phenomenon is known as tension stiffening. In other words, tension stiffening is a phenomenon about the effect of the concrete under tension on rebars in the distance between two consecutive cracks. In the crack location, all tensile force is resisted by the reinforcement material. However, a part of the tensile force is transferred to the concrete through the bond action between cracks. The phenomenon reduces the stresses and strains of the reinforcement material and results in a mean strain of the reinforcement material less than the reinforcement material in the crack area. Therefore, the concrete increases the stiffness of the reinforcement material in the distance between cracks, and the effective elasticity modulus of the reinforcement material is increased.

Figure 1 shows the way that axial force is distributed between concrete and rebar and also indicates the effect of the development of cracks on the force distribution between concrete and rebar. As it is observed from figure 1, while the tensile force applied in member, the applied force in rebar is transferred to the surrounding concrete through the bond between rebar and concrete. The contribution of the concrete and rebar from applied force to the member depends on their stiffness. In this stage, the stress distribution is uniform along the member, for rebar and concrete. As the force applied to the member increases, the stresses applied to the rebar and concrete increase until the stresses of the concrete reach their cracking strength. In this stage, the first crack appears in the concrete around the rebar. According to figure 1b, as crack develops in the concrete, the stress tolerated by the concrete in the crack location tends to be zero. Thus, the stresses increase in the rebar around the crack. According to figure 1b, all stresses are beard by the rebar in the crack location and the range that it is called transfer length. As move further than the crack location, stress is decreased in the rebar until the stress distribution is uniform. The increase in the force applied to the member makes the stress of the concrete reach its cracking strength along the member and finally, it results in crack development in the concrete. According to figure 1c, the increase in the number of cracks results in the increase in the areas of non-uniform stress distribution (transfer length) along the member under tension. The process reduces the concrete's contribution to the resistance of the tensile force. Finally, almost all applied force is resisted by the rebar in the final loading stage. Figure 2 shows the process of force resistance by rebar and concrete in a

specimen under tension as in figure 1. As it is observed, there is no crack in the first part of the curve with a linear behaviour, and the force applied to the member is distributed between concrete and steel uniformly. However, 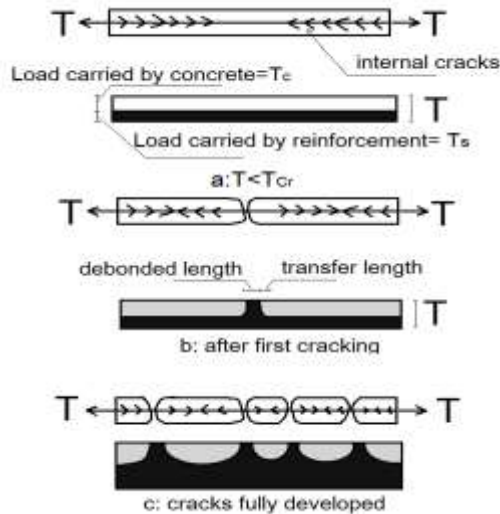after the crack developed, there is no balance in the force distribution between concrete and rebars. In the last part of the curve with many cracks in the specimen, almost all force is resisted by the rebar as in figure 2 [3].
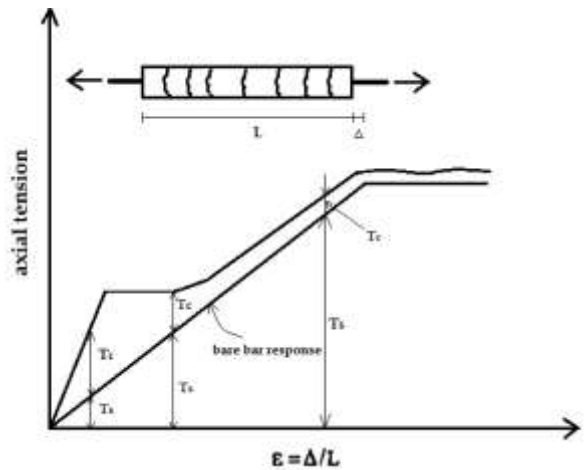

Fig. 1. Force distribution between concrete and reinforcement [3].

Fig. 2. Force-strain curve of the reinforced concrete member under tension [3].

3. Experimental Program

To achieve the purposes of the research, 24 specimens of cylindrical reinforced concrete with the length 1000 mm and a center rebar is prepared. A direct tension test is performed on all specimens. The test specimens are classified into four groups with different rebar materials. The purpose of the classification is to investigate the effect of rebar strength on tension stiffness. In any test groups, two rebar diameters 12 and 16 are used to evaluate the effect of changes in the rebar diameter on the tension stiffening behaviour. Also, cover thickness is chosen for any test specimen in a way that the C/d ratios (ratio of the concrete cover thickness of the rebar to the rebar diameter) 1.5, 2, 2.5,

3, 4 and 5 are obtained for the specimens. C/d ratios are chosen in order to evaluation of the effect of the concrete cover thickness and reinforcement ratio ($\rho = A_s/A_c$) on the tension stiffening behaviour of the ultra-high performance concrete. In fact, the effect of important parameters is evaluated on the tension stiffening behaviour of the concrete by designing suitable experiments.

3. 1. Property of Materials

The materials used to prepare the test specimens is include ultra-high performance concrete, steel rebars and Glass Fiber Reinforced Polymer (GFRP) rebars. In this section, the mechanical properties of ultra-high performance concrete, steel rebars and GFRP rebars are introduced.

3.1.1. Ultra-High Performance Concrete

Ultra-high performance concrete is composed of Portland cement, quartz powder, silica fume, silica sand, superplasticizer and water. High strength cement type 1 is used to make the concrete, and the water to cement ratio is 0.2. The mixing design of the concrete is presented in table 1. After studying different proportions of the materials, this mixing design provides the maximum compressive strength. The mechanical properties are presented in table 2 based on the related standard experiments.

3.1.1.1. Mixing process

Firstly, the dry materials mixed to achieve a homogeneous mixture .This can take several minutes. Then part of the water and half of the superplasticizer add to mix. Mixing will continue until the materials completely combine. In the next step, the remaining water and superplasticizer add to mix.

3.1.1.2. Material properties

Ultra-High Performance Concrete constituent materials are Portland cement, Silica fume, Quartz powder, Silica sand, superplasticizer and water.
The physical properties of the aggregates, used for this work, is described as follow:

Table 1. UHPC mix proportions

Materials	kg/m^3
Cement	670
Quartz powder	285.0
Silica fume	200.0
Silica sand	1020.0
Superplasticizer (3%)	20.1
Water	178.0

- Quartz powder

Quartz powder is an essential material in Ultra-High Performance Concrete. Average diameter of its particles is 0.01 mm. Quartz powder is a hard material that improves the properties of the matrix.

- Silica sand

Sand particle size is limited to 0.8 mm, but not less than 0.15 mm. Silica sand has advantages such as high hardness and easy access.

- Super Plasticizer

Since the water-cement ratio is very low for the Ultra-High Performance Concrete, carboxylate-based Plasticizers is used to increase the workability of fresh concrete.

Table 2. Mechanical properties of UHPC

Mechanical properties	value
Compressive strength (MPa)	110.00
Modulus of elasticity (GPa)	41.18
Density (kgf/m3)	2100.00
Splitting tensile strength of cylindrical Specimens (MPa)	10.51
Direct Tensile strength (MPa)	9.00

3.1.2. Steel Rebars

Steel rebars are used as reinforcement in some specimens. The tensile stress of the yield point and modulus of elasticity of steel rebars are obtained by tension test based on DIN EN10002 Standard [11]. The mechanical properties of steel rebars based on experimental results are presented in table 3.

3.1.3. Glass Fiber Reinforced Polymer (GFRP) Rebars

GFRP rebars have lateral surfaces with a weak rib. To ensure the mechanical properties provided by the factory, the tension test was performed on specimens of GFRP rebars. GFRP is a non-homogeneous material and its features are different in different orientations. Therefore, the tension test specimen should be prepared in a way that rebars are not crushed under compressive stresses of connectors. For this purpose, specimens were prepared according to ACI 440.3R Code [4]. GFRP rebars were fixed inside steel pipes. Then, the pipes were filled with resin. To prevent the slip between the resin and the smooth surface of the pipe, the inner part of the steel tube is grooved to provide the required roughness. The mechanical properties of the standard experiments of GFRP rebars are given in table 4.

Table 3. Average mechanical properties of steel rebars.

Mechanical properties	Rebar type	
	AII	AIII
Modulus of elasticity (GPa)	214.5	219.5
Yield strength (MPa)	399.18	478.00
Yield strain (mm/mm)	0.00233	0.00225
Ultimate strength (MPa)	571.00	663.00
Failure strain (mm/mm)	0.2584	0.2513

Table 4. The average mechanical properties of GFRP rebars.

Mechanical properties	Test specification	
	GFRP1	GFRP2
Ultimate strain %	1.76	1.74
Ultimate stress (MPa)	1190	1037
Modulus of elasticity (GPa)	66	54

3.2. Specimens Preparation

3.2.1. Preparation of the Steel-Reinforced Specimens

12 specimens were prepared from UHPC and steel rebars. The specimens have circular sections and 1000 mm length. A steel rebar is put at their center as the reinforcement. and protrudes 150 mm from both sides of the specimen to hold it in the testing setup. (Figure 3). In the specimens, rebars with the diameters 12 and 16 are used for reinforcement. The outer diameters of the cylindrical concrete specimens are selected 65 mm, 100 mm and 150 mm to provide the desired C/d ratios. Two types of AII and AIII steel rebars are used to evaluate the effect of the features of the rebar, including the strength and modulus of elasticity on the tension stiffening behaviour of the concrete specimen.

3.2.2. Preparation of GFRP Reinforced Specimens

12 specimens were prepared from UHPC and GFRP rebar. Their specifications are similar to steel reinforced specimens and only the type of rebar has changed. Two different GFRP rebars are used instead of the steel rebar. Since GFRP rebars are weak against the surrounding pressure, special conditions must be met to connect the specimens to the tension test device. For this purpose, some steel pipes must be used at both ends of the rebar so that the adhesive resin in casings controls the rebar. The length of the casings is 350 mm proportional with the load-carrying capacity of the rebars, and the inner surface of the casings is grooved to prevent from the slip between the resin and the inner surface of the casing. Details of the specimens are presented in figure 4.
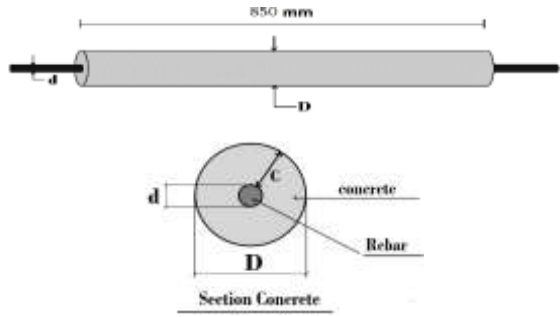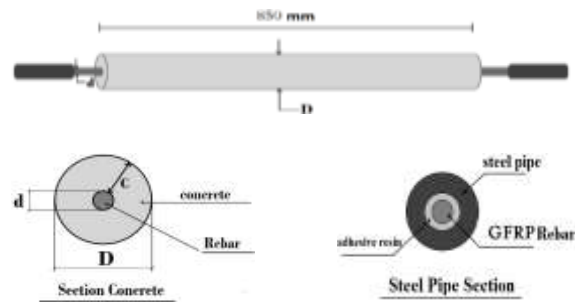
Fig. 3. Test specimens of UHPC and steel rebars


Fig. 4. Test specimens of UHPC and GFRP rebar

3.3. Experimental Setup

After preparing and curing, the tension test is performed on all specimens; that way, the tensile force is applied to the rebar by a hydraulic jack. The force applied to the rebar, is transferred to its surrounding concrete through the bond between concrete and rebar. Four LVDTs are used at the top and bottom the specimens on the rebar and concrete to transfer the displacements to the data logger. Force-displacement curves of both ends of specimens are drawn from the recorded data. The changes in the specimen's stiffness, its load-carrying capacity and the effect of cracks development on the structural behaviour can be evaluated using the force-displacement curve obtained from the experiments at different loading levels. Figure 5a and 5b show test setup and several specimens after cracking.
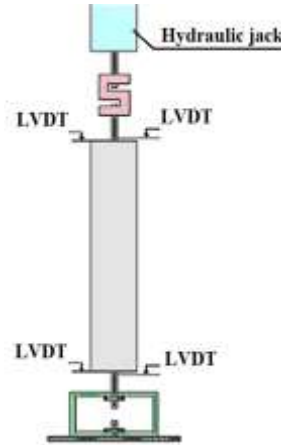
LVDT: Linear Variable Differential Transformer

Fig. 5a. Test Setup.

Fig. 5b. Specimens after cracking.

3.4. Naming of Specimens

Specimens are named in a way that their physical and geometrical features are identified quickly. The general pattern is X-Y-M, where X is concrete specimen's diameter, Y is rebar's diameter, and M is the type of rebar. For example, 65-16-AII represent a concrete specimen with the diameter 65 mm that is reinforced with an AII steel rebar of 16 mm diameter at the center of the specimen. General specifications of specimens are given in table 5.

4. Tensile Stress-Strain Behaviour of the Specimens and their Parameters.

4.1. Average Stress-Strain Curve of Specimens

Experiments are designed to examine the effect of concrete cover thickness, reinforcement ratio and type of rebar on the behaviour of the reinforced concrete specimens. Average tensile stress-strain curves of all specimens are given at figures 6 and 7. Comparing the initial stiffness of the specimens (stiffness of specimens before crack development), it can be found that the increasing thickness of the concrete cover is resulted to increase the initial stiffness so that for specimens reinforced with both AII and AIII steel rebars, the initial stiffness increases 4.5, 5.5 and 7.5 times more than the rebar stiffness (with no cover), for specimens with outer diameter of 65 mm, 100 mm and 150 mm, respectively.

The curves in figure 6 show that the change in the type of rebar from AII to AIII has been decreased the initial stiffness before crack development in all specimens with similar reinforcement ratio and cover thickness (due to the similar diameter of the specimen and the rebar). For specimens with a higher reinforcement ratio, such as the specimens 65-12-(AII, AIII) and specimens 65-16-(AII, AIII), there is a 9% decrease. However, for the specimens 150-16-(AII, AIII) and 150-12-(AII, AIII) with a minimum reinforcement ratio, there is a 5% decrease, and there is a 12% decrease for the specimens 100-12-(AII, AIII) and 100-16-(AII, AIII). In two specimens with same diameters, the increase in the rebar diameter, that leads to an increase in the reinforcement ratio (ρ), has decreased the stiffening effect and the increase in the initial stiffness before the development of the first crack for both AII and AIII rebars. In similar specimens, the increase in the reinforcement ratio has led to an increase in the force resistance capacity of the member. On the other hand, the increase in the reinforcement ratio has decreased the concrete cross-section around the rebar in two specimens with similar diameters. The decrease in the concrete cross-section has made the concrete reach its tensile strength sooner and its effect on the member stiffness has decreased as the crack developed. Hence, the increase in the reinforcement ratio has reduced the tension stiffening effect. On the other hand, the increase in the specimen diameter for a similar rebar type has increased the concrete cross-section around the rebar, and it reaches the tensile capacity later for an equal concrete force with the higher diameter. It decreases the number of cracks and increases the initial stiffness and the stiffening effect. The study of the behaviour of the specimens after crack development shows that in specimens with a lower cover thickness, as consecutive cracks

develop, the stiffness decrease in the tensile strain-stress curve of the specimens is not sharp. However, in specimens with a higher thickness of the concrete cover on the rebar, such as in specimens with the outer diameter

150 mm, development of consecutive cracks in the specimens has created a steep slope in the stiffness decrease in the stress-strain curve.
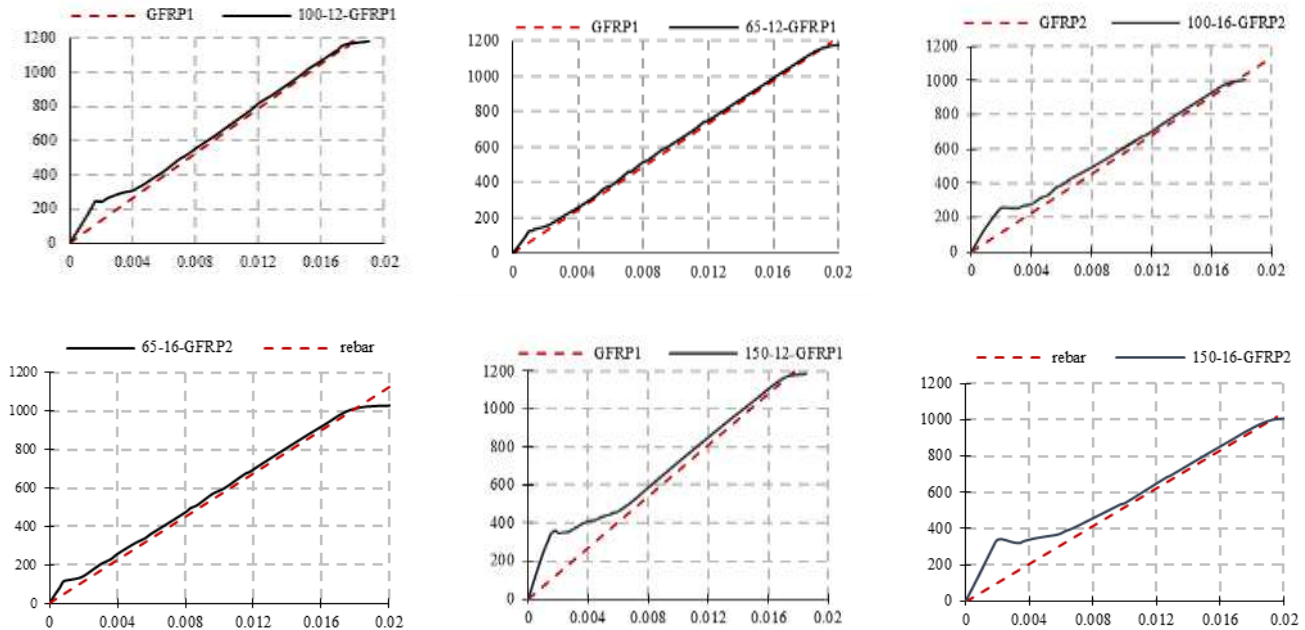

Figure 6. Stress-strain curve for same of the specimens reinforced with GFRP rebar (in all curves, the vertical axis is the stress (MPa) and the horizontal axis is the strain (mm/mm)).

In specimens with a large concrete cover thickness, the stability stage of the crack is very short due to the failure of rebar after the development of cracks. However, after the stage of crack development, the cracks become stable and their width increases for specimens with a low concrete cover thickness such as in specimens with the outer diameter 100 mm, and especially for specimens with the outer diameter 65 mm. The phenomenon is observable in the figures of the previous sections. The reason can be interpreted with regarding the strength of the steel bars, as it is not possible to continue the crack stability stage in the specimen with the high cover thickness or low reinforcement ratio, and rebar failure occurs.

The curves in figure 6 show that the initial stiffness of the specimens (the specimens' stiffness before cracking) is two times more than the rebars with no concrete cover (for specimens with the diameter 65 mm reinforced with GFRP1 and GFRP2 rebars with the diameters 12 and 16 mm). In addition, it is 2.6 times more than the rebars with no cover in specimens with the outer diameter 100 mm (for both diameters and both types of rebars), and it is 3.5 times more than the rebars with no cover in specimens with the diameter 150 mm. The values show that as the specimen's diameter increases, or as the thickness of the concrete cover on the rebar increases, the initial stiffness increases. However, the increase in the stiffness of the specimens reinforced with GFRP rebars before cracking is less than in the specimens

reinforced with steel rebars so that it is 3 times less in the specimens with the outer diameter 150 mm, and is 2 times less in specimens with the outer diameter 65 mm. The behaviour of the specimens reinforced with GFRP rebars after cracking shows that the cracks are stable and open in all specimens. In specimens with a lower concrete cover thickness, especially in specimens with the outer diameter 65 mm, the development of the consecutive cracks with a mild slope has decreased the specimen's stiffness. However, the decrease in the stiffness is more for specimens with the outer diameter 150 mm due to the development of the consecutive cracks. Comparing both GFRP and steel-reinforced specimens, it is observed that after cracks develop, the decrease in the specimen's
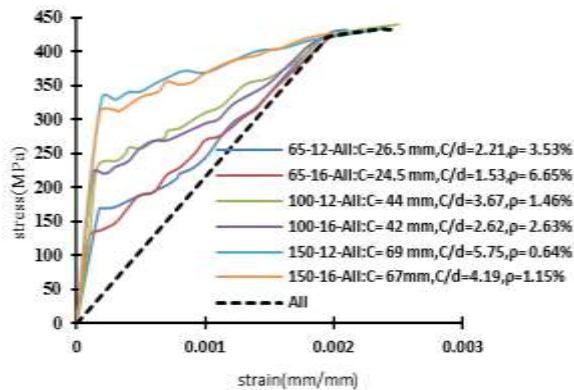
stiffness is smaller in the specimens reinforced with GFRP rebars than in the specimens reinforced with steel rebars.

4.2. Parameters Affecting the Average Tensile Stress-Strain Behaviour of the Specimens

The stress-strain curves in the previous section show that different factors including the type of the rebar, the reinforcement ratio of the specimen and the concrete cover thickness are the most critical factors affecting the behaviour of the test specimens. Hence, the effect of the change in the concrete cover on the rebar is examined for each type of rebar. The effect of type of rebar is evaluated for similar concrete cover thicknesses and reinforcement ratios in figures 7 and 8.
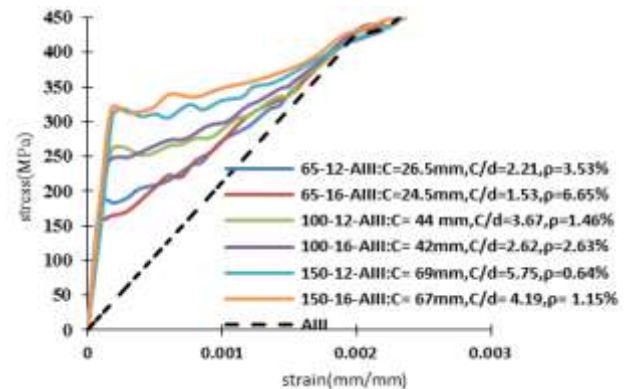

Fig. 7a. Stress-strain curve of the specimens reinforced with AII rebar.

Fig. 7b. Stress-strain curve of the specimens reinforced with AIII rebar.

The curves in figure 7a show that in AII reinforced specimens, the increase in the thickness of the concrete cover and consquently decrease in the reinforcement ratio led to an increase in the initial stiffness of the specimens and the intensity of the cracks' development (increase in the tensile stress of the specimen that creates the first crack in the concrete). The reason is that the stress transfers from the rebar to the concrete

due to the bond between the concrete and rebar in the test specimens. The transferred stress makes the specimen crack and the crack develops radially from the rebars. The increase in the thickness of the concrete cover on the rebar increases the path the cracks must follow to reach the specimen's surface. Hence, more force is needed to create the crack. For the reinforced specimens with AII rebar with a higher outer

diameter, as the crack develops in the specimen, the curve's slope decreases sharply after the cracks develop. According to the curves in figure 7b, the increase in the concrete cover thickness has increased the initial stiffness for the specimens reinforced with AIII rebar. Unlike the specimens reinforced with AII rebar, if the rebar's diameter changes from 12 to 16 (that increases the reinforcement ratio) in the specimens reinforced with AIII rebar and identical diameter, the stiffness is slightly affected before crack. However, the initial stiffness increases as the reinforcement ratio increases at similar specimens reinforced with AII rebar with the outer diameters 65 mm and 100 mm. The reason of the fact that the initial stiffness of the specimens reinforced with AIII rebar does not change as the reinforcement ratio changes compared to the specimens reinforced with AII rebar can be attributed to the nature of AIII rebar. In fact, it can be said that the lower ductility and the higher strength of the rebar affect the behaviour. In all specimens reinforced with AIII rebar, as the reinforcement ratio and the thickness of the concrete cover have

increased, crack development has resulted in a sharp decrease in the slope of the curve after cracking. However, compared to the specimens reinforced with AII rebar, the reduction in the slope is not sharp. In fact, specimens with AII rebar have a higher reduction in the stiffness. The reason can be attributed to the higher ductility of AII rebar compared to AIII rebar. The stress-strain curves of the tensile behaviour of the specimens reinforced with GFRP1 and GFRP2 rebars in figure 8a and figure 8b indicate that as the thickness of the concrete cover increases, the initial stiffness of the specimen's increases. However, the increase in the stiffness is much less than the specimens reinforced with steel rebars. In most specimens reinforced with GFRP rebar, the stress of the crack development is higher than in similar specimens reinforced with steel rebars. In all specimens reinforced with both types of GFRP rebars, cracks become stable after they develop. Whereas, the same situation occurs only in the specimens with a high reinforcement ratio (lower cover thickness) reinforced with steel rebars.

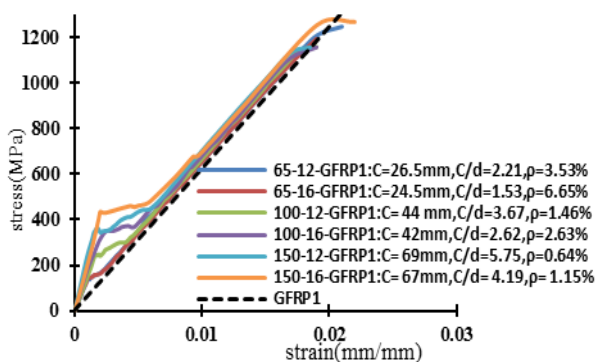**Fig. 8a.** Stress-strain curve of the specimens reinforced with the GFRP1 rebar.

Fig. 8b. Stress-strain curve of the specimens reinforced with the GFRP2 rebar.

For specimens with identical outer diameter for both GFRP rebars, in after stage of the genesis of initial cracks, the increase in the
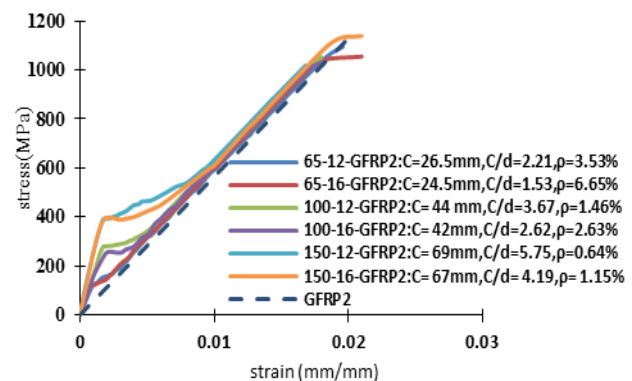
rebar diameter is caused to slow down the decrease in the stiffness of the specimens, as the number of the cracks increased.

However, the reduction is smaller than the steel-reinforced specimens. In the specimens reinforced with GFRP1, the change in the reinforcement ratio of the specimens with identical outer diameter has increased their initial stiffness as the reinforcement ratio increased. However, the phenomenon did not occur for the specimens reinforced with GFRP2. The curves in figure 8 show that increment in the reinforcement ratio has increased the required force for the development of the first crack in similar specimens, but the increase in force for GFRP1 reinforced specimens is more than of that for GFRP2 reinforced specimens. Comparison between the curves of figures 7 and 8 shows that in all curves, the stiffness of the steel reinforced specimens is significantly more than that of GFRP reinforced specimens.

The increase in stiffness is more provided for specimens with a lower outer diameter and consequently, with a higher reinforcement ratio such as specimens by 65 mm outer diameter. The decrease in the stiffness of the similar specimens reinforced with GFRP rebars is reduced after the stage of development of the cracks. The sharp decreasing the stiffness is evident between steel and GFRP rebars specimens with a lower cover thickness. After the stage of crack development, the decrease in the stiffness is similar in the 150 mm outer diameter specimens reinforced with 12mm and 16mm rebars and in the 100 mm outer diameter specimens reinforced with 16mm rebar.

In all specimens reinforced with steel rebars and different reinforcement ratios, the strain of the first crack (the beginning of the crack development) is 8 to 10 times less than that in the specimens reinforced with GFRP

rebars. The failure stress and strain of all AIII reinforced specimens are similar to the failure stress and strain of the AII reinforced specimens , and there is no difference. However, in the specimens reinforced with GFRP rebar, the failure strain is similar for both types of the rebars GFRP1 and GFRP2, but the failure stress of the specimens reinforced with GFRP1 rebar is 8-10% more than the failure stress of the specimens reinforced with GFRP2.

4.3. Tensile Stress-Strain Curves of the Concrete Contribution

If the tensile force T is applied to the specimen, the following equation of equilibrium obtained for each segment.

$$T = F_S + F_C \tag{1}$$

In the recent equation, F_s is the average rebar contribution tensile force, that is obtained as follows:

$$F_S = A_S E_S \varepsilon_{sm} \tag{2}$$

ε_{sm} is the average strain of the rebar along the reinforced concrete specimen that is obtained from the experiment for any force T. E_s and A_s are modulus of elasticity and cross-section of the rebar, respectively.

The average of the concrete contribution tensile force is obtained by equation 3:

$$F_C = T - F_S \tag{3}$$

The average tensile stress of the reinforced concrete specimen is obtained from the following equation:

$$\sigma_{cm} = \frac{F_C}{A_C} \tag{4}$$

Where, A_c is the concrete cross-section ($A_c = A_g - A_s$).

Regarding the equation 4, the variations of the average concrete tensile stress are obtained in terms of the average rebar strain. This equation is very useful in the nonlinear analysis of the reinforced concrete structures using the finite element method and taking the smeared crack model into account.

The variation curve of the tensile strength of concrete contribution (σ_{cm}) is indicated in figure 9, in terms of the average strain of the rebar (ε_{sm}) for some specimens. The curves in figure 9 show that stress increases linearly with strain for all specimens before the crack development. After crack development, it decreases nonlinearly. The comparison of the curves of the specimens reinforced with GFRP rebar and the specimens reinforced with steel rebar shows that the decrease in the descending branch of GFRP reinforced specimens is sharper than the steel reinforced specimens. In the specimens reinforced with

both steel and GFRP rebars, the increase in the outer diameter has reduced the crack tensile stress in the specimens, because of the concrete's cross-section increases, resulting in a higher tensile force. In the specimens with the similar outer diameter and rebar diameter, the change in the type of rebar, i.e. from steel rebar to GFRP rebar, has decreased their crack tensile stress from 25 to 30%. Since steel rebars have a larger stiffness (modulus of elasticity) than GFRP rebars, and the steel rebar resists a larger force in an equivalent strain, more force is transferred to the concrete and the tensile stress of the concrete increases when the specimens crack. In similar specimens, the change of the type of the rebar from AII to AIII does not largely affect the concrete crack stress. However, in the specimens reinforced with AIII rebar, the decrease in the descending branch is a little more than the specimens reinforced with AII rebar. The trend is evident in the specimens reinforced with GFRP1 rebar compared to the specimens reinforced with GFRP2 rebar.
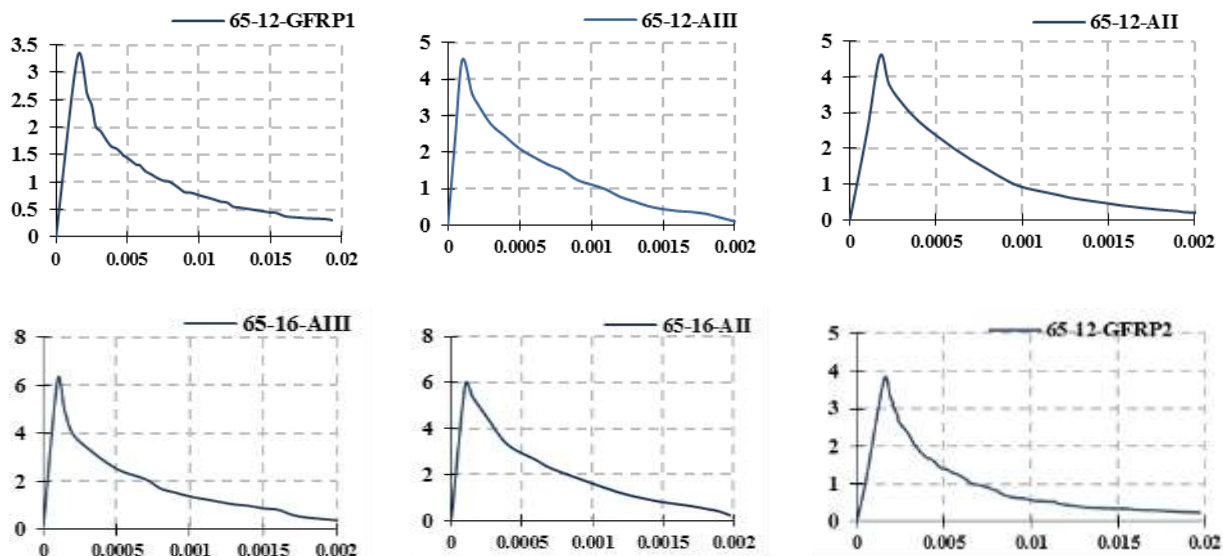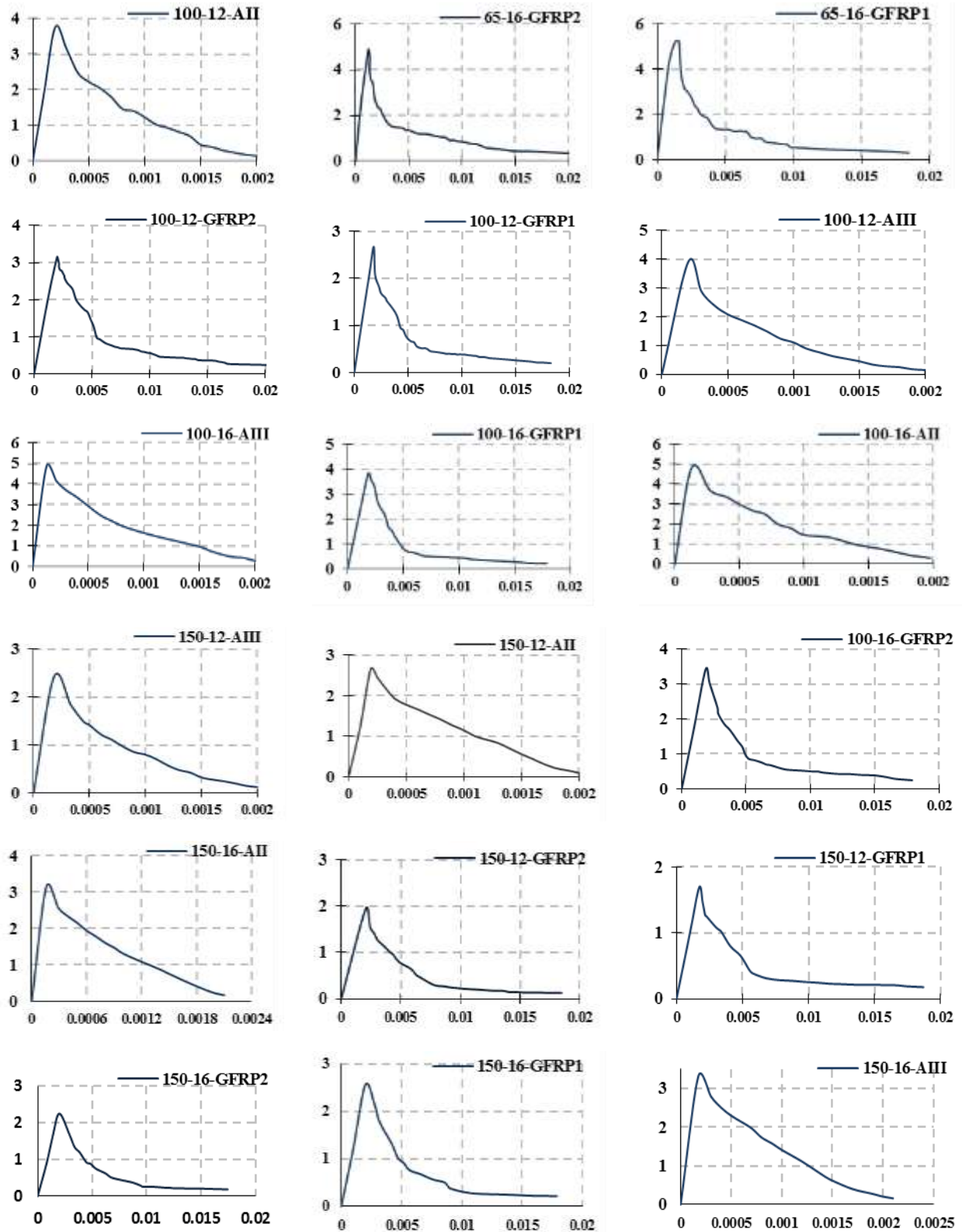
Fig. 9. Tensile stress-strain curves of the concrete contribution for some different specimens (in all above curves, the vertical axis is the stress (MPa) and the horizontal axis is the strain (mm/mm)).

5. A Tension Stiffening Model for UHPC

To obtain a suitable model for tension stiffening behaviour of the ultra-high performance concrete, we first normalize the tensile stress-strain curve of the concrete presented in the previous section. For this purpose, we divide data of the strain axis by the crack strain of the specimen, and divide the tensile stress axis by the crack stress of the specimen in all curves so that dimensionless curves are obtained. A linear relation is offered between the ratio of stresses and strains before crack development. Since the post-cracking behaviour of all specimens is like a nonlinear descending branch, the equation (5) is proposed for the post-cracking behaviour of ultra-high performance concrete.

$$\frac{\sigma_t}{\sigma_t^{cr}} = \alpha e^{-\beta \left(\frac{\varepsilon_t}{\varepsilon_t^{cr}} \right)} + \gamma \tag{5}$$

In this equation, σ_t is the tensile stress of the concrete after crack development, $\sigma_{cr}{}^t$ is the tensile crack stress of the concrete, ε_t is the strain equivalent to σ_t and $\varepsilon_{cr}{}^t$ is the crack strain. The parameters α, β, γ are proportional to the geometrical properties of the specimen and the way that they are obtained is described in the next section.

The parameters α, β, γ are given in table 5. the R^2 (Coefficient of determination) of the data is above 0.99, showing an excellent compliance between the model and the test results. Hence, the reinforced concrete behaviour includes two parts: linear behaviour before cracking and nonlinear behaviour after cracking (equations 5 and 6). In the first area, the relation between stress

and strain is linear. The area continues until the stress reaches the concrete's tensile strength.

$$\sigma_t = \left(\frac{\sigma_t^{cr}}{\varepsilon_t^{cr}} \right) \varepsilon_t \tag{6}$$

In the second area, after cracking begins in the specimen, the stress that the concrete can resist decreases exponentially, and its behaviour is as follows based on the test results.

In these equations, σt is the tensile stress of the concrete after cracking, σcrt is the crack tensile stress of the concrete, εt is the strain equivalent to σt and εcrt is the crack strain. The various factors affect the parameters α, β, γ including the type of the rebar, C/d ratio, nρ and other different factors. Hence, to obtain the best relation for any parameter, multivariate regression is used based on their factors. The relations obtained for the parameters α, β, γ are given in the equations 7 to 9.

The Coefficient of determination (R^2) of the above equations are 0.92, 0.90 and 0.80, respectively, showing the suitable compliance between the equations and the test results.

6. Conclusions

The purpose of the present research was to study the tension stiffening behaviour of ultra-high performance concrete and to propose a model for the post-cracking behaviour of the concrete in the reinforced concrete members under tension or in the tensile region of the reinforced concrete member using steel and GFRP rebars. For this purpose, the direct tension test was performed on 24 UHPC specimens

reinforced with steel and GFRP rebars. By analyzing the experimental data and the proposed equations, the following results are obtained:

Table 5. Model parameters based on the statistical analysis of the test results.

No.	Specimen	Cover.	C/d*	Reinf. ratio (ρ)%	α	β	γ
1	65-12-AIII	26.5	2.2	3.53	1.064	0.163	0.012
2	65-12-AII	26.5	2.2	3.53	1.304	0.346	0.026
3	65-12-GFRP1	26.5	2.2	3.53	1.134	0.365	0.11
4	65-12-GFRP2	26.5	2.2	3.53	1.101	0.497	0.082
5	100-12-AIII	44	3.65	1.46	1.275	0.312	-0.012
6	100-12-AII	44	3.65	1.46	1.303	0.260	-0.051
7	100-12-GFRP1	44	3.65	1.46	1.785	0.819	0.106
8	100-12-GFRP2	44	3.65	1.46	1.710	0.588	0.095
9	150-12-AIII	69	5.75	0.64	1.253	0.256	-0.012
10	150-12-AII	69	5.75	0.64	1.535	0.115	-0.426
11	150-12-GFRP1	69	5.75	0.64	1.675	0.684	0.109
12	150-12-GFRP2	69	5.75	0.64	1.844	0.768	0.063
13	65-16-AIII	24.5	1.53	6.45	1.008	0.229	0.095
14	65-16-AII	24.5	1.53	6.45	1.116	0.167	0.032
15	65-16-GFRP1	24.5	1.53	6.45	1.842	0.895	0.116
16	65-16-GFRP2	24.5	1.53	6.45	1.668	0.806	0.114
17	100-16-AIII	42	2.62	2.63	1.157	0.152	-0.024
18	100-16-AII	42	2.62	2.63	1.180	0.145	-0.053
19	100-16-GFRP1	42	2.62	2.63	2.573	0.985	0.085
20	100-16-GFRP2	42	2.62	2.63	2.162	0.893	0.111
21	150-16-AIII	67	4.20	1.15	1.412	0.126	-0.277
22	150-16-AII	67	4.20	1.15	1.319	0.115	-0.224
23	150-16-GFRP1	67	4.20	1.15	1.953	0.727	0.082
24	150-16-GFRP2	67	4.20	1.15	1.973	0.765	0.082

* C/d: Ratio of cover thickness to rebar diameter

$$\alpha = -0.831 - 34.67n\rho + 0.287C - 0.002C^2 - 2.19\frac{C}{d} + 0.196\left(\frac{C}{d}\right)^2 + 516.5\frac{n\rho}{C} + 177.81\frac{n\rho}{d} \tag{7}$$

$$\beta = -4.13 - 24.1n\rho - 0.0005C^2 + 0.283d + 0.7\frac{C}{d} + 344.54\frac{n\rho}{C} + 116.63\frac{n\rho}{d} \tag{8}$$

$$\gamma = +0.311 - 3.88n\rho + 5.15n\rho^2 - 0.0063C + 0.01d + 34.55\frac{n\rho}{C} \tag{9}$$

- In the specimens reinforced with steel rebars, the increase in the concrete cover thickness is increased the initial stiffness of the specimens about 4.5, 5.5 and 7.5 times for both AII and AIII reinforced specimens with outer diameter of 65 mm, 100 mm and 150 mm compared to specimens without cover, respectively.

- The increase in the specimen's diameter and consequently increase in the thickness of the concrete cover lead to an increase in initial stiffness. However, before cracking, the increase in the initial stiffness of specimens reinforced with GFRP rebars is lower than those of specimens reinforced with steel rebars.

- The post-cracking behaviour of the specimens reinforced with GFRP rebars shows that the stability and opening crack stage is completed in all specimens. Comparing the specimens reinforced with GFRP rebars with those reinforced with steel rebars, it is observed that the decrease in specimen's stiffness after crack development is smaller in the specimens reinforced with GFRP rebars than those reinforced with steel rebars.

- In all specimens reinforced with steel rebars and different reinforcement ratios, the strain of the first crack (the beginning of the crack development) is 8 to 10% less than the crack strain in the specimens reinforced with GFRP rebars. The stress and it's corresponding strain of the specimens reinforced with AIII steel rebar are somewhat similar to those in the AII rebar. However, in the specimens reinforced with GFRP rebar, the failure strain is similar for both GFRP1 and GFRP2 rebars. But the failure stress of the specimens reinforced with GFRP1 rebar is 8 to 10% more than

that in the specimens reinforced with GFRP2.

- The coefficients of determination (R^2) are obtained more than 0.90; thus the suitable correlation is provided between the proposed models and the experimental data.

REFERENCES

[1] Richard, P., Cheyrezy, M. (1995). "Composition of reactive powder concretes." Cement and Concrete Research 25(7): 1501-1511.

[2] Abbassi, M.,Dabbagh, H. (2014). "Behaviour of FRP-Confined Reactive Powder Concrete Columns under Eccentric Loading." Journal of Rehabilitation in Civil Engineering 2(1): 46-64.

[3] Abrishami, H. H., Mitchell, D. (1996). "Influence of splitting cracks on tension stiffening." ACI structural journal 93(6): 703-710.

[4] ACI, A. (2004). "440.3 R-04: Guide Test Methods for Fiber-Reinforced Polymers (FRPs) for Reinforcing or Strengthening Concrete Structures." American Concrete Institute, Farmington Hills, USA.

[5] Akbarzadeh Bengar, H., Yavari, M. R. (2016). "Simulation of the Reactive Powder Concrete (RPC) Behaviour Reinforcing with Resistant Fiber Subjected to Blast Load." Journal of Rehabilitation in Civil Engineering 4(1): 63-77.

[6] Garber, D., & Shahrokhinasab, E. (2019). Performance Comparison of In-Service, Full-Depth Precast Concrete Deck Panels to Cast-in-Place Decks (No. ABC-UTC-2013-C3-FIU03-Final). Accelerated Bridge Construction University Transportation Center (ABC-UTC).

[7] Shahrokhinasab, E. (2019). ABC-UTC Guide for: Full-Depth Precast Concrete (FDPC) Deck Panels.

[8] Baena, M., Torres, L., Turon, A., et al. (2013). "Analysis of cracking behaviour and tension stiffening in FRP reinforced concrete tensile

elements." Composites Part B: Engineering 45(1): 1360-1367.

[9] Darwin, D., Scanlon, A., Gergely, P., et al. (1986). "Cracking of concrete members in direct tension." ACI committee 224: 224.222R221-224.222R212.

[10] Deng, Z.-C., Jumbe, R. D., Yuan, C.-X. (2014). "Bonding between high strength rebar and reactive powder concrete." Computers and Concrete 13(3): 411-421.

[11].DIN EN 10002, (1991). "Tensile Testing of Metallic Materials- Part 1: Method of Test at Ambient Temperature", DIN- Adopted European Standard.

[12] Ebead, U. A., Marzouk, H. (2005). "Tension-stiffening model for FRP-strenghened RC concrete two-way slabs." Materials and Structures 38(2): 193-200.

[13] Eligehausen, R., Popov, E. P., Bertero, V. V. (1982). Local bond stress-slip relationships of deformed bars under generalized excitations. 7th European Conference on Earthquake Engineering, Athens,Greece.

[14] Ghalehnovi.Mansour (2004). Constitutive Relationships in Nonlinear Analysis of RC Structures Considering effects of Bond-Slip and Corrosion. PhD, University of Science and Technology.

[15] Lee, G.-Y.,Kim, W. (2009). "Cracking and Tension Stiffening Behaviour of High-Strength Concrete Tension Members Subjected to Axial Load." Advances in Structural Engineering 12(2): 127-137.

[16] Marzouk, H.,Chen, Z. (1995). "Fracture energy and tension properties of high-strength concrete." Journal of Materials in Civil Engineering 7(2): 108-116.

[17] Nematzadeh, M., Poorhosein, R. (2017). "Estimating properties of reactive powder concrete containing hybrid fibers using UPV." Computers and Concrete 20(4): 491-502.

[18] Rahdar, H.,Ghalehnovi, M. (2016). "Post-cracking behaviour of UHPC on the concrete members reinforced by steel rebar." Computers and Concrete 18(1): 139-154.

[19] Saleem, M. A., Mirmiran, A., Xia, J., et al. (2012). "Development length of high-strength steel rebar in ultrahigh performance concrete." Journal of Materials in Civil Engineering 25(8): 991-998.

[20] Shirmardi, M. M., Mohammadizadeh, M. R. (2019). "Numerical Study on the Flexural Behaviour of Concrete Beams Reinforced by GFRP Bars." Journal of Rehabilitation in Civil Engineering 7(4): 88-99.

[21] Stramandinoli, R. S. B., La Rovere, H. L. (2008). "An efficient tension-stiffening model for nonlinear analysis of reinforced concrete members." Engineering Structures 30(7): 2069-2080.

[22] Tang, C.-W. (2017). "Uniaxial bond stress-slip behaviour of reinforcing bars embedded in lightweight aggregate concrete." Struct. Eng. Mech 62(5): 651-661.

[23] Yoo, D.-Y., Banthia, N., Yoon, Y.-S. (2016). "Flexural behaviour of ultra-high-performance fiber-reinforced concrete beams reinforced with GFRP and steel rebars." Engineering Structures 111: 246-262.